文章编号：1001-9014(XXXX)XX-0001-08

DOI:10.11972/j.issn.1001-9014.XXXX.XX.001

Strongly coupled electro-optical tunable 780 nm ultra-narrow linewidth laser source

XUE Kai[2], RONG Jia-Min[2*], XING Guo-Hui[2], XUE Jun-Jie[1], LIU Wen-Yao[1], ZHOU Yan-Ru[1], XING En-Bo[1], TANG Jun[2], LIU Jun[1]

(1. Key Laboratory of Electronic Testing Technology, School of Instrument and Electronics, North University of China, Taiyuan 030051, China;
2. School of Semiconductors and Physics, North University of China, Taiyuan 030051, China)

Abstract: Highly matched and precisely locked to the absorption lines of rubidium (Rb) atoms, 780 nm lasers play a crucial role in fields such as quantum computing, precision measurements, and high-sensitivity sensing, with clear requirements for strong coherence and fast tunability. In this paper, based on the self-injection locking and ultra-high quality factor whispering gallery mode (WGM) cavity, a 780 nm narrow linewidth (23.8 kHz) tunable laser with a single longitudinal mode output is verified. More importantly, benefiting from the optimized combined coupling coefficient K and via the lithium niobate electro-optic effect, the laser frequency detuning is effectively improved, with the experimental tuning range reaching 110 pm and the tuning efficiency of 6.4 pm/V. This work provides a high-performance design solution for fast-tunable narrow-linewidth lasers for applications in the near-infrared range, which is expected to play an essential role in the future.

Key words: rubidium, whispering gallery mode, lithium niobate, self-injection locking, wavelength tunability

强耦合电光可调谐 780nm 超窄线宽激光源

薛 凯[2], 戎佳敏[2*], 邢国徽[2], 薛俊洁[1], 刘文耀[1], 周彦汝[1], 邢恩博[1], 唐 军[2], 刘 俊[1]

(1. 中北大学仪器与电子学院电子测试技术重点实验室,山西 太原 030051;
2. 中北大学半导体与物理学院,山西 太原 030051)

摘要:780 nm激光器频率可以高度匹配并精确锁定到铷(Rb)原子吸收线上,对强相干性和快速可调谐性有着明确的要求,从而在量子计算、精密测量和高灵敏度传感等领域起到关键作用。本文基于自注入锁定线宽压窄效应,得益于回音壁谐振腔超高品质因子,验证了780 nm自注入锁定窄线宽可调谐激光器,并实现十千赫兹量级(23.8 kHz)的单纵模输出。更重要的是,通过优化组合耦合系数K,结合铌酸锂电光效应,有效提高激光器频率失谐度,调谐范围达到110 pm,调谐效率为6.4 pm/V。该研究为近红外范围内应用的快速调谐窄线宽激光器提供了高性能的设计方案,有望在未来发挥重要作用。

关 键 词:铷原子;回音壁模式;铌酸锂;自注入锁定;波长调谐

中图分类号:O436 **文献标识码**:A

Introduction

Narrow linewidth tunable lasers have been extensively utilized in the fields of quantum sensing[1], quantum computation[2] and quantum communication[3] due to their advantages, including high precision, excellent stability, long coherence times and significant nonlinearity[4]. These features are particularly beneficial for laser frequency locking of ^{87}Rb atoms[5]. Specifically, the transitions from $5S_{1/2}$ to $5D_{5/2}$ and from $5S_{1/2}$ to $5P_{3/2}$ states

Received date: 2024-12-17, **revised date**: 2025-01-15 **收稿日期**:2024-12-17,**修回日期**:2025-01-15

Foundation items: General Program of National Natural Science Foundation of China (62373331), Joint Funds of the National Natural Science Foundation of China (U21A20141), Innovative Research Group Project of the National Natural Science Foundation of China (51821003), Natural Science Foundation of Shanxi Province (202403021211095).

Biography: XUE Kai (2000-), male, Lvliang, master. Research area involves Self-injection locking lasers. E-mail: 1633824270@qq.com.

* **Corresponding author**: E-mail: rongjiamin@126.com

of ^{87}Rb atoms occur at wavelengths of 778.1 nm and 780.2 nm, respectively, leading to the formation of corresponding absorption spectra[6]. Lasers are crucial in this context, not only by providing a precise laser source for atomic transitions but also by offering a tunable feature that enables the adjustment of specific wavelengths to coincide with the rubidium absorption lines. This alignment ensures that the photon energy perfectly matches the energy levels of the atomic transitions. Furthermore, the accuracy and stability of the experiment are significantly enhanced through the application of frequency locking and cooling technologies. The absorption spectrum width of ^{87}Rb atoms at room temperature typically spans the megahertz (MHz) range; however, it can be narrowed to the 10 kHz to 100 kHz range through the use of cryogenic cooling techniques combined with the Doppler effect[7]. Consequently, the availability of fast, tunable, narrow linewidth lasers operating at the 10 kHz level is particularly crucial[8].

Tunable narrow linewidth lasers are predominantly based on external cavities, typically utilizing the self-injection locking technique. In this approach, a portion of the laser′s output is fed back into the cavity, interacting with the laser-generated modes and thereby locking the laser′s output frequency to the cavity′s resonant frequency, which establishes a stable and synchronized state[9]. External cavities employed for self-injection locking of semiconductor lasers include high-quality factor Fabry－Pérot (FP) cavities, grating external cavities, WGM cavities, and fiber-coupled external cavities. Among these, WGM cavities demonstrate a very high quality factor and small mode volume across a wide wavelength range, making them an ideal platform for external cavity self-injection locking lasers[10]. Notably, lithium niobate (LN) exhibits a significant Pockels effect and serves as an excellent dielectric material for implementing electro-optical modulation techniques[11-12]. To achieve linewidth narrowing and wavelength tunability for 1550 nm self-injection locking lasers, Lin et al. (2022) utilized an erbium ion-doped LN cavity, achieving a final linewidth of 322 Hz and a high tuning efficiency of 50 pm/100 V[13]. In 2023, Cheng et al. employed a photolithography-assisted chemo-mechanical etching (PLACE) technique to fabricate an LN cavity, successfully realizing a 980 nm narrow linewidth laser output, with the linewidth narrowed to 10.9 GHz and a wavelength tunable range of 2.57 nm[14]. In the same year, John E. Bowers′ team achieved a linewidth narrowing of a distributed-feedback (DFB) pumping laser to 4.7 kHz at 780 nm using a thin-film lithium niobate cavity with self-injection locking[15].

Conventional laser tuning techniques typically rely on current or temperature regulation, and in some cases, they require complex external feedback systems. FP external cavities adjust the free spectral range (FSR) by varying the distance between the external cavity mirrors, thereby tuning the laser output wave[16]. The cavity length usually determines the upper limit of its tuning range. While increasing the cavity length can enhance the FSR, thereby extending the tuning range, it also leads to an increase in the external cavity volume, which can adversely affect the stability and operational efficiency of the laser. Wavelength tuning of fiber bragg grating depends on changes in temperature or strain to adjust the reflected wave of the grating[17]. This method necessitates precise temperature control; particularly in scenarios with significant temperature fluctuations, the tuning accuracy may be considerably compromised. The tuning method proposed in this paper involves appropriate increase of the distance between the laser and the cavity, in conjunction with applying a voltage directly to the WGM cavity, which effectively avoids the limitations caused by increasing the cavity length of the external cavity. This study has the advantage of combining theoretical analysis and practical application. We derived the analytical equation of the locked bandwidth based on the linewidth narrowing theory, explicitly established the relationship between optical parameters and the locked bandwidth, and revealed the influence of these factors on the wavelength tuning range of the laser by optimizing the Q value of the external cavity and the light propagation time delay, effectively adjusting the frequency detuning degree, and thus extending the tuning range of the laser.

Although high-Q WGM cavities offer substantial advantages in linewidth narrowing[18-19], the tunable range correspondingly decreases as their linewidth narrows. This paper presents a derivation of an analytical equation for the locked bandwidth, based on the theoretical framework of linewidth narrowing[20]. In our experiments, we achieved the self-injection locking of a 780 nm laser using a LN cavity with a Q factor of 2×10^6. The narrow linewidth of the laser, measured using short delayed self-heterodyne interferometry, is 23.8 kHz[21-24]. Additionally, through the electro-optic effect, the narrow linewidth laser exhibits a wavelength tunable range of 110 pm and a tunable efficiency of 6.4 pm/V. To investigate the self-injection locking technique, the experiment was carried out in the near-infrared band at 780 nm, thus convincingly demonstrating the great potential of the technique for laser linewidth narrowing and wavelength tunability.

1 Experiment

1.1 Self-injection locking

This model illustrates a laser cavity composed of an FP cavity (consisting of two mirrors) effectively demonstrates the self-injection locking mechanism, see Fig. 1 (a). The laser emitted by the diode is focused by a lens and coupled into the cavity through a prism. The cavity′s dimensions and surface roughness can induce backward Rayleigh scattering, with some of the scattered laser being fed back into the laser cavity. This self-injection effect enhances the interaction between the signal from the laser cavity and the external cavity. The interaction occurs when the laser source signal aligns with the cavity signal, locking the output frequency of the laser to that of the optical signal in the external cavity, thereby achieving linewidth narrowing. As shown in Fig. 1(b), during the initial phase of the self-injection locking experiment, the output mode of the laser does not match with the cavi-

ty mode, leading to a multimode output spectrum. By adjusting the positional relationship between the laser and the cavity, as well as the coupling spacing, mode matching is gradually achieved, successfully realizing the self-injection locking effect. Subsequently, the output mode of the laser is precisely locked to the fundamental mode of the cavity, resulting in a single-mode output state.

Fig. 1 (a) Self-injection locking schematic. In the figure, prism coupling feeds back a portion of the laser beam back into the laser cavity to achieve self-injection locking. (b) The cavity mode is gradually matched to the laser mode, and the single-mode output after self-injection locking and the significant linewidth narrowing phenomenon reflect the optimization effect of the mode matching. (c) The corresponding tunable ranges of cavities at different radii and thicknesses

In this experiment, the LN cavity is successfully prepared using diamond cutting and mechanical polishing techniques. This cavity has a diameter of 5 mm and a thickness of 0.2 mm, Fig. 3(b) shows the top view of the prepared resonator under an optical microscope. We measure the Q factor of the cavity using the full width at half maxima method with a 1550 nm laser, and the Q factor of the cavity reached 10^6 in the critical coupling case. Through theoretical analysis, the bandwidth adjustment mechanism of WGM laser under self-injection locking condition is revealed, and the analytical formula for the locked bandwidth is[20]:

$$\xi = \zeta + \frac{K}{2}\frac{2\zeta\cos\bar{\psi} + \left(1+\beta^2-\zeta^2\right)\sin\bar{\psi}}{\left(1+\beta^2-\zeta^2\right)+4\zeta^2}\ , \tag{1}$$

where ξ and ζ denote the frequency detuning of the laser to the cavity and the output frequency detuning, respectively; β is the normalized backscattering coefficient; $\bar{\psi}$denotes phase-locked ; K is the combined coupling coefficient, which is analogous to the injection parameter C used in the theory of self-mixing interferometers, as depicted in the following equation[25]:

$$C = \left(1+\alpha^2\right)^{1/2} A^{-1/2}\kappa s/n_{las}L_{las}\ , \tag{2}$$

Where

$$\kappa = \varepsilon\delta(1-R)/\sqrt{R}\ , \tag{3}$$

The function denotes the fraction of the field coupled back and interacting with the laser mode. In Eqs. (2) and (3), α is the linewidth enhancement factor of the laser, $1/A$ is the fraction of power fed back into the laser, s is the distance from the laser to the cavity, and the measured value is s = 6 cm, in addition, n_{las} and L_{las} are the effective refractive index and the cavity length of the laser, respectively, and ε is the mode superposition factor, δ is the diffusivity (if not already included in A) typically reflecting the degree of scattering of laser reflected from the surface, and R is the cavity reflectivity. In the design of cavities, there is an important relation between

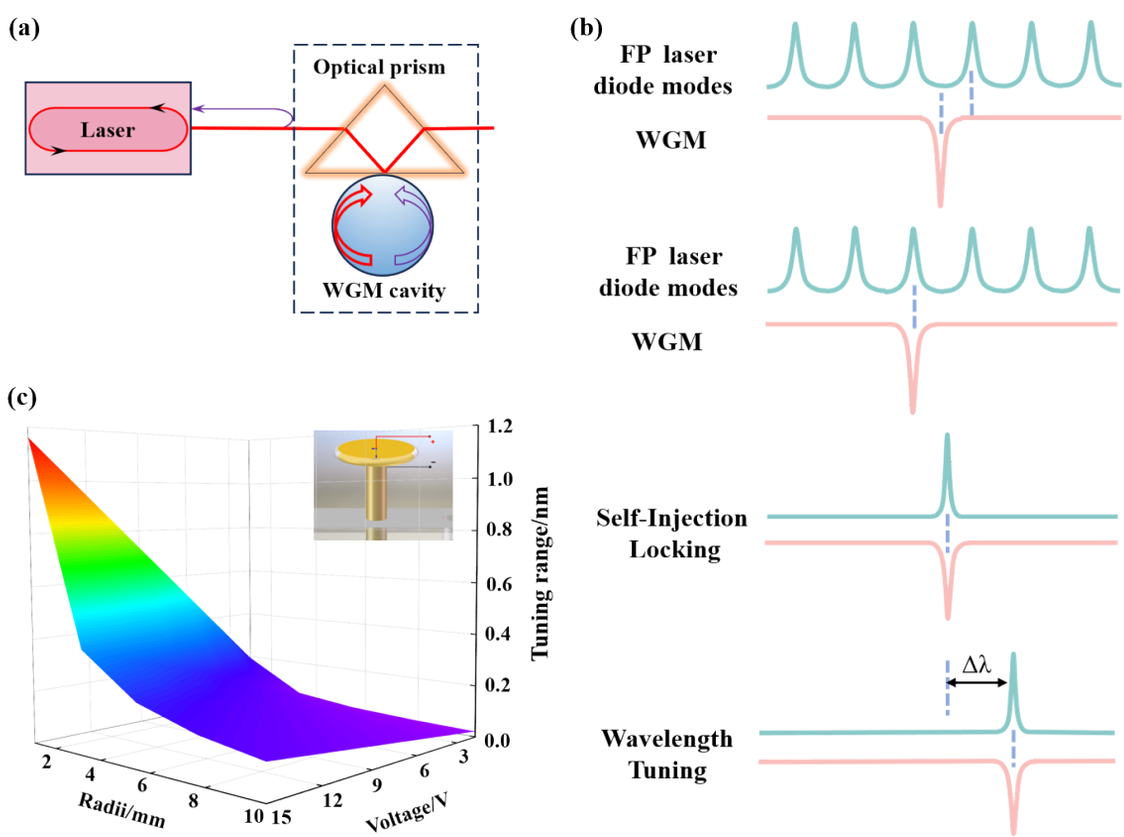

图 1　(a) 自注入锁定原理图,采用棱镜耦合技术。图中,棱镜耦合将激光束的一部分反馈回激光器腔内,实现自注入锁定。(b) 谐振腔模式与激光器模式逐渐匹配,自注入锁定后的单模输出且线宽的显著压窄现象,反映了模式匹配的优化效果。(c)不同半径和厚度下的谐振腔对应的调谐范围

the reflectivity R and the quality factor Q, which is displayed in the following equation[26]:

$$R = \exp\left(-\frac{t_r}{2\tau}\right), \tag{4}$$

where $t_r = 2L/c$ denotes the time required for the laser to round-trip through the cavity, and by combining Eqs. (2), (3), and (4) and substituting the relevant parameters, the relationship between C and Q is expressed as:

$$C = 80\left[\exp(5 \times 10^4 Q^{-1}) - \exp(-5 \times 10^4 Q^{-1})\right], \tag{5}$$

From Eq. (5), the injection parameter C increases as the quality factor Q decreases, while the combined coupling coefficient K increases, similar to that in Eq. (1). Furthermore, as indicated in Eq. (1), the value of K affects the frequency detuning between the laser and the cavity, and the larger value of K results in greater detuning, which subsequently enhances the wavelength tunable range of the laser. In this experiment, we use a lithium niobate cavity with a quality factor Q of 2.3×10^6. We intentionally select a lower Q for the cavity because appropriately reducing the Q value allows us to maintain the narrow linewidth characteristics of the laser while simultaneously increasing its tunable range. This enhancement increases the adaptability of the laser system to the diverse needs of various applications, thereby enhancing its versatility and practicality. As shown in Eq. (2), the distance between the laser and the cavity affects the tunable range of the self-injection locking laser. Compared to on-chip self-injection locking lasers, our design incorporates a relatively greater distance between the laser and the cavity, allowing for a further extension of the laser's tunable range.

Figure 2 (a) illustrates the self-injection locking bandwidth tuning curve derived from the optimized of Eq. (1). The figure demonstrates that as the indicated laser frequency is scanned from the redshift to the resonant frequency of the WGM cavity, the output frequency of the laser jumps to within the self-injection locking bandwidth as the frequency difference between the two decreases. Within this locking bandwidth, the output frequency of the self-injection locking laser remains essentially constant. The locking bandwidth describes the frequency range over which the laser can be stabilized after being locked by an external feedback system (e. g., an external reference laser) and a larger locking bandwidth means that the laser can remain stable over a wider frequency range. The linewidth compression factor based on the WGM laser self-injection locking technique is shown in Eq. (6)[27]:

$$\frac{\delta\omega}{\delta\omega_{free}} \approx \frac{Q_d^2}{Q^2}\frac{1}{16\Gamma_m^2\left(1+\alpha_g^2\right)}, \tag{6}$$

where $\delta\omega$ and $\delta\omega_{free}$ are the laser linewidths based on WGM self-injection locking and the laser linewidths in the free-running state, respectively; Q_d (10^2) and Q (10^6) are the quality factors of the laser cavity and the external LN cavity, respectively; Γ_m and α_g denote the reflection coefficient as well as the phase-amplitude coupling coefficient of the cavity, respectively. According to this formula, the order of magnitude of the linewidth compression factor is 10^8, which leads to a theoretically calculated linewidth value of 19 kHz, and the experimental laser linewidth measured by the short delayed self-heterodyne interferometry is 23.8 kHz.

Through the optimization of relevant parameters, the one-to-one correspondence between the combined

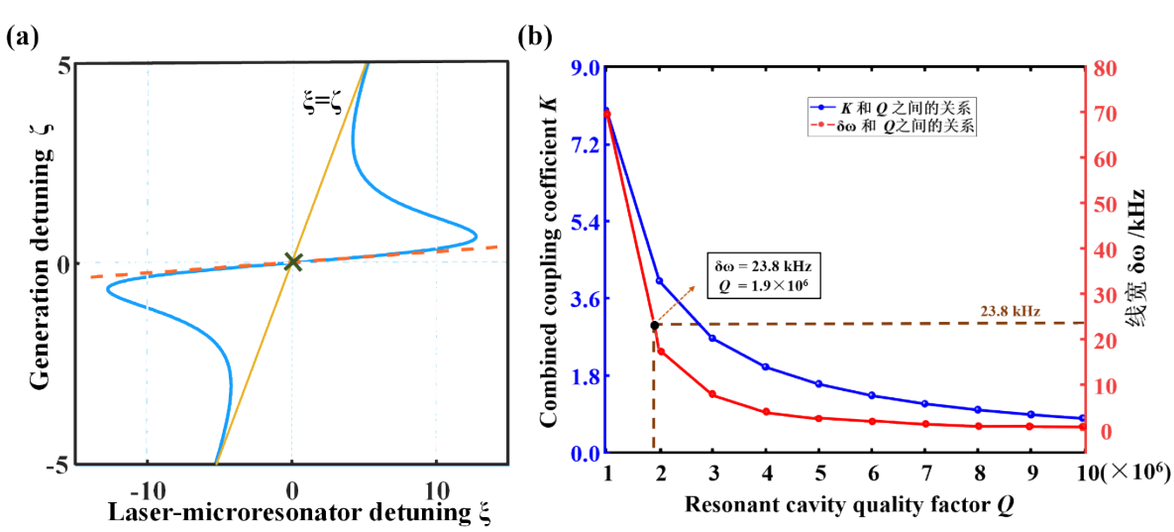

Fig. 2 (a) Based on WGM laser self-injection locking bandwidth tuning. When the laser frequency is tuned away from the resonant frequency of the cavity, the laser generation frequency follows the 1:1 line, marked in orange in the figure. As the laser frequency approaches the resonance of the cavity, it gradually stabilizes until it jumps to the stable center portion of the curve, which is marked with a red line in the figure. (b) One-to-one correspondence of the combined coupling coefficient K and linewidth δ_ω with the cavity quality factor Q, respectively

图 2 (a) 基于WGM激光自注入锁定带宽调节曲线图。当激光频率被调谐远离谐振腔的谐振频率时,激光产生频率遵循1:1线,图中用橙色标注。当激光频率接近谐振腔共振时,逐渐稳定,直至跳到曲线的稳定中心部分,图中用红线标注。(b) 组合耦合系数K、线宽δω分别与谐振腔品质因子Q的一一对应关系

coupling coefficient K and linewidth $\delta\omega$ with the cavity quality factor Q, respectively, is shown in the equation of Fig. 2(b). The achievable parameters and their corresponding specific values for the WGM and laser cavity selected for the experiment are provided in Table 1.

As shown in Fig. 3(a), a high-precision three-dimensional electric displacement stage is used to discretely regulate the microcavity-prism coupling spacing with an accuracy of 20 nm, enabling precise control of the coupling state, coupling strength and backscattered light power. The laser chip is selected from a commercial FP laser model HLM40105-C component. The commercially available FP chips for laser modules are coated with a highly transmissive film on the output side and a highly reflective film on the input side. The air cooling device and current drive of the component are necessary in the experimental setup. The tunable focusing lens in the laser assembly is difficult to verify the self-injection locking effect and is removed in the experimental setup. The 780 nm light (the laser chip-based) is focused by an optical focusing mirror with an NA value of 0.53 to the first side end face of the coupling prism, which is fully reflected by the prism to form evanescent field and coupled to the cavity. The coupled output light exits through the second side end face of the coupling prism and is collected by the focusing fiber. Among them, the optical focusing mirror, coupling prism on both sides of the wall is coated with 780nm band permeability enhancement film to avoid interference of the reflected light on the laser chip, to ensure that the Rayleigh scattering is the main reason for realizing the self-injection locking.

1.2 Short delayed self-heterodyne interferometry

Since the laboratory is equipped with a spectral analyzer that has a resolution of 0.05 nm, and the linewidth resulting from self-injection locking is much narrower than 0.05 nm, directly measuring the laser's specific linewidth with the spectroscope is challenging. Therefore, the present experiment adopts the short delayed self-heterodyne interferometry to measure the narrow linewidth of the 780 nm self-injection locking laser. This method determines the laser linewidth by analyzing pairs of data points (i.e., adjacent maxima and minima) in the signal generated by the self-heterodyne device. The structure of the short delayed self-heterodyne interferometry measurement linewidth device is depicted in Fig. 4(a). The output of the measured laser is split into two beams by coupler 1 (50:50): one beam is frequency shifted by an acousto-optic modulator (AOM) with a center frequency of 100 MHz, this process helps differentiate the laser signal from its self-referenced frequency, thereby reducing system noise and errors caused by laser frequency drift and environmental changes[24], thus ensuring stability and reliability. The other laser beam is delayed through a 150 m single-mode fiber. The two beams are then recombined and injected into the photodetector (PD) via coupler 2 (50:50). Finally, we measure the beat-frequency signals of the two beams using a spectrum analyzer. When the fiber delay time τ_d is smaller than the laser coherence time τ_c, the power spectrum of the beat signal shows a distinct narrow peak at the operating frequency of the AOM. As the ratio of the laser coherence time to the fiber delay time (τ_c/τ_d) increases, the

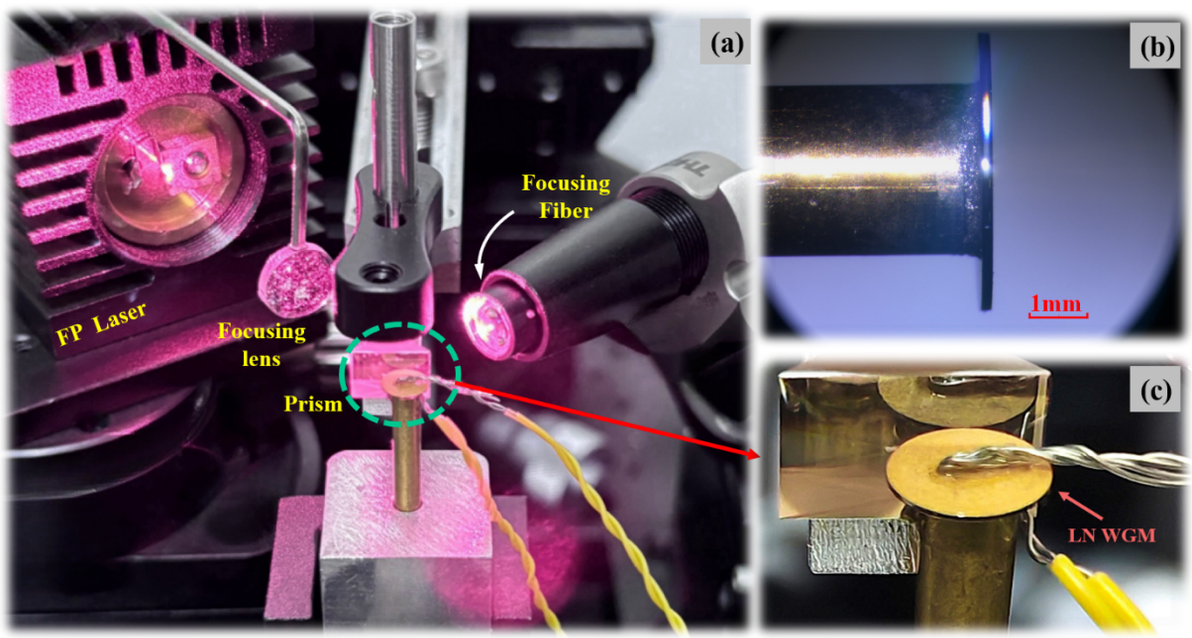

Fig. 3 (a) Schematic diagram of the self-injection locking experimental equipment. The figure contains the main components: the laser, the prism, the LN cavity, and the fiber at the receiving end (which collects and transmits the optical signals passing through the cavity). (b) Top view of the polished cavity under an optical microscope. (c) Enlarged view of the area shown by the green box in Fig. 3(a)

图3 (a) 自注入锁定实验设备示意图。图中包含主要组件:激光器、棱镜、谐振腔以及接收端光纤(收集和传输经过谐振腔的光信号)。(b) 光学显微镜下抛光谐振腔的俯视图。(c) 图3(a)中绿框所示区域的放大图

signal-to-interference plus noise ratio (SINR) of the peak of the differential beat signal centered at the AOM frequency increases monotonically.

Table 1 Parameters related to WGM and laser cavity
表 1 与 WGM 和激光器谐振腔有关的参数

Parameter name	Notation	Value
Linewidth enhancement factor	α	2.5
Fraction of power fed back into the laser	*1/A*	0.01
Effective refractive index of the laser	n_{las}	3.5
Laser cavity length	L_{las}	50 μm
Mode superposition factor	ε	0.4
Diffusivity	δ	0.2
Cavity reflection coefficient	Γ_m	10^{-2}
Cavity phase-amplitude coupling factor	α_g	0.5

Among them, 1/A, ε, δ, α_g are taken according to the critical coupling state and combined with the actual experiments; α, Γ_m are taken from Ref. 27, n_{las}, L_{las} are fixed values after the selection of a suitable laser.

During the linewidth measurement, the difference between the values of the vertical axis at a pair of extreme points is taken for calculation purposes. The relation between ΔS and Δf can be constructed when τ_d and f are known. τ_d is controlled by the length of the fiber, and f can be taken as the value of the frequency at the envelope extremes, and the computational relationship can be expressed as[22]:

$$\Delta S = 10\log_{10}S_H - 10\log_{10}S_L, \tag{7}$$

where S_H and S_L are pairs of extreme points on the envelope. ΔS denotes the amplitude difference between the two extreme points, and the period τ_d can be expressed in terms of the fiber length as

$$\tau_d = nL/c, \tag{8}$$

where n is the refractive index of the fiber and L is the fiber length. According to the period τ_d, the difference between the frequency at the extreme point and the center can be deduced as:

$$\Delta f_m = (m+2)c/2nL, \tag{9}$$

where m is a natural number, if $m = 0$ at the extreme point closest to the center frequency (minimum value), $m = 1$ at the second extreme point closest to the center frequency (maximum value), and so on. By combining Eqs. (7) and (9), the relations between Δf and ΔS can be expressed as:

$$\begin{aligned}\Delta S &= 10\log_{10}S_H - 10\log_{10}S_L \\ &= 10\log_{10}\frac{S[f_1+\frac{(m+2)c}{2nL}]}{S[f_1+\frac{(k+2)c}{2nL}]} \\ &= 10\log_{10}\frac{[\Delta f^2+[\frac{(k+2)c}{2nL}]^2][1-\exp(-2\pi\frac{nL}{c}\Delta f)\cos[(m+2)\pi]]}{[\Delta f^2+[\frac{(m+2)c}{2nL}]^2][1-\exp(-2\pi\frac{nL}{c}\Delta f)\cos[(k+2)\pi]]},\end{aligned} \tag{10}$$

where S_H is the larger of the neighboring extreme points, S_L is the smaller of the neighboring extreme points, m and k are natural numbers. Since this is a pair of neighboring extreme points, the condition $|m-k| = 1$ must be satisfied.

In this experiment, we connect 150 m of delayed fiber to the test setup. This modulator focuses the beat frequency at 100 MHz, avoiding the interference from environmental factors in the experiment. As a result, the signal within the critical test frequency paradigm (i. e., 100 MHz) remains stable for a long time, even though the ambient noise causing the PSD to fluctuate in the low-frequency band near 0 Hz. Figure 4(b) shows that within the swept frequency range, a pair of extreme points are selected for numerical analysis and combined with Eq. (10). The result obtained from the first-order and second-order extreme points (m = 0, k = 1) is 23.8 kHz. The laser output power is gradually increased from 6 mW to 13 mW, allowing us to explore the effect of laser power on laser linewidth. During the experiment, a set of coherent envelope data is recorded for each 1 mW increment, and the corresponding linewidth is calculated, as shown in Fig. 4(d). It can be clearly seen from the figure that the measured laser linewidth decreases as the increase of laser output power. When the laser power is increased to 13 mW, the measured laser linewidth reaches its minimum value of 23.8 kHz. The true linewidth of the laser itself narrows within the low power range of 6 mW to13 mW. From the one-to-one correspondence illustrated in Fig. 4(c), it can be concluded that when conducting short delayed self-heterodyne interferometry to measure the narrow linewidth of a laser, the precise linewidth can be determined from the actual measured peak-to-valley difference (ΔS) and the specific length of the delayed fiber, once the length of the delayed fiber has been selected.

1.3 Wavelength tunable

Self-injection locking lasers with tunable wavelength are highly selective and stable, offering a wide range of prospects in optical applications. in this process, the wavelength tuning of a self-injection locking laser is achieved by adjusting the voltage applied to the LN cavity. The refractive index of LN changes significantly under the action of an electric field due to its significant electro-optical effect. The upper and lower surfaces of the LN cavity are coated with a gold-plated layer approximately 150 nm thick, which not only improves the conductivity of LN but also ensures the uniformity of the electric field distribution through the metal electrodes. In the LN cavity, the upper and lower metal-plated surfaces are

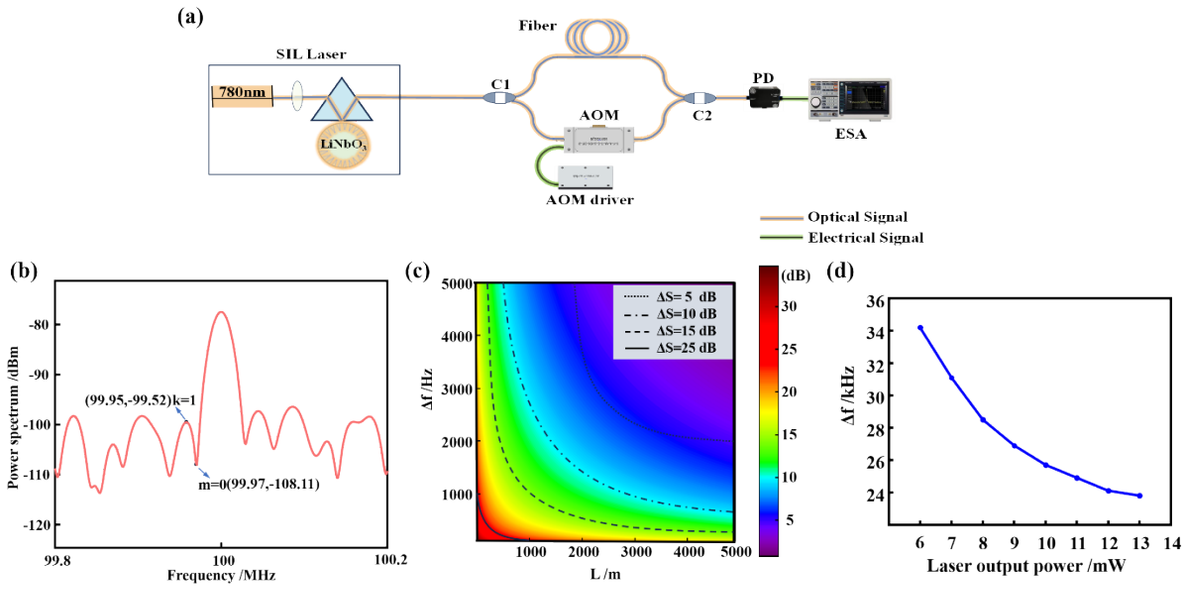

Fig. 4　Measured laser linewidth for the short delayed self-heterodyne interferometry. (a) C1 and C2: optocoupler (50/50). The delayed fiber length is 150 m. PD: photoelectric detector. AOM: acousto-optic modulator (100 MHz). ESA: electronic spectrum analyzer. (b) Plot of the envelope data for the delayed fiber length of 150 m used. (c) Magnitude difference between a pair of extreme points corresponding to different delayed fiber lengths (L) and laser linewidth (Δf). (d) Laser linewidth corresponding to different laser power
图4　短光纤延迟自外差法的测激光线宽。(a) C1和C2:光耦合器(50/50)。延迟光纤长度为150米。PD:光电探测器。AOM:声光调制器(100MHz)。ESA:电子频谱分析仪。(b)使用的延迟光纤长度为150米的包络数据图。(c) 不同延迟光纤长度(L)和激光线宽(Δf)所对应的一对极值点的幅度差。(d) 不同的激光器功率对应的激光线宽

connected to electrodes, and a direct current voltage source is connected between the plane electrodes on the LN surface, creating a bias voltage, as shown in Fig. 3(c).

In this research, we investigate the variation of a laser′s wavelength in continuous tuning mode. The smooth variation of the laser wavelength across a continuous range is achieved by voltage-tuning the optical properties of the cavity. As illustrated in Fig. 5(a), when a voltage ranging from 0V to 18V is applied to the cavity, the laser wavelength shifts from 787.83 nm to 787.94 nm. This results in a tunable range of 110 pm, corresponding to a wavelength tunable efficiency of 6.4 pm/V. During the examination of the laser′s tunable characteristics at various applied voltages, we incrementally adjust the voltage and simultaneously record the corresponding spectrograms. The side-mode suppression ratio (SMSR) is also calculated, as shown in Fig. 5(c). The SMSR of these spectrograms was analyzed and found to vary over a range of 5.1 dB at different voltages. This range indicates that, although there is some fluctuation in the RMSR, the overall variation is within an acceptable range, suggesting that the laser maintains relatively stable performance during the tunable process. Differences in the tunable range correspond to varying cavity sizes, therefore, we analyze the impact of the size factor on the tunable

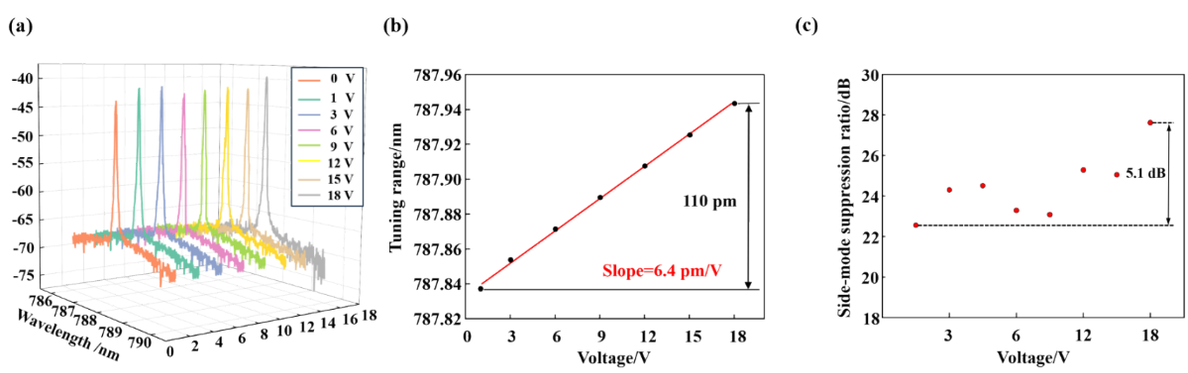

Fig. 5　Wavelength tunable plot of a 780 nm self-injection locking laser. (a) Spectra of laser output power at different applied voltage levels to the cavity. (b) Narrow linewidth laser wavelength versus applied voltage to the cavity. The linear fit (red curve) shows a slope of 6.4 pm/V. (c) Side-mode suppression ratio of the spectra with different voltages applied to the cavity
图5　780nm自注入锁定激光器波长调谐图。(a) 谐振腔不同外加电压水平下激光器输出功率的光谱。(b) 窄线宽激光波长与谐振腔外加电压的关系。线性拟合(红色曲线)显示斜率为6.4pm/V。(c) 谐振腔施加不同电压下光谱的边模抑制比

range, as illustrated in Fig. 1(c). When the radius of the LN cavity is less than 3 mm, the curve rises rapidly, indicating that this region is the one with the largest change in tunable range. In contrast, the remaining area shows less variation and a reduced tunable range. The tuning voltage applied to the LN cavity is proportional to the tunable range when the radius no longer changes. By adjusting the laser power to achieve wavelength tunability, the effectiveness of this tunable range is contingent upon variations in power. This necessitates frequent adjustments to the laser power; however, such changes can induce thermal effects, potentially leading to an increase in the laser's temperature, which may adversely affect its performance. Consequently, the tuning method used in this experiment is more precise and offers greater reference value for future research on the wavelength tunability of self-injection locking lasers.

2 Conclusions

In summary, we demonstrate a high-performance narrow-linewidth laser operating at 780 nm is demonstrated, achieving exceptional performance through self-injection locking of the FP laser into a high-Q LN WGM cavity. In this study, we have achieved a laser linewidth of 23.8 kHz, which meets the 10 kHz linewidth requirement for cooled ^{87}Rb atoms. This matching has been shown to enhance the interaction efficiency between the laser and the cooling atoms, leading to improved cooling efficiency and a greater degree of cooling. Furthermore, the laser demonstrates significant tunability, with a wavelength tunable range of approximately 110 pm and a tunable efficiency of 6.4 pm/V. This paper also examines the change in the root mean square ripple (RMSR) during the tunable process, which has been accurately measured at approximately 5.1 dB. This indicates the relative stability of the laser. During course of the experiments, the laser wavelength is continuously tuned, and this method achieves finer wavelength tuning compared to directly adjusting the laser power. This tuning approach effectively mitigates the thermal effects caused by high power, preventing mode jumping and ensuring stable laser output. By optimizing the relevant parameters, a cavity with an appropriate quality factor Q is selected, which further extends the laser's tunable range and iimproves its tuning efficiency. These improvements not only enhance laser performance but also lay the groundwork for the future development of high-precision laser technologies.

References

[1] Wang Y, Zhang Y, Li C, et al. Stable Single-Mode 795 nm Vertical-Cavity Surface-Emitting Laser for Quantum Sensing[J]. Materials, 2024,17(19):4872-4872.

[2] Artem Prokoshin, Weng W. Chow, Bozhang Dong, Frederic Grillot, John Bowers, Yating Wan; Linewidth narrowing in self-injection locked lasers: Effects of quantum confinement[J]. APL Photonics 2024,9(8):086106.

[3] Otterpohl A, Sedlmeir F, Vogl U, et al. Squeezed vacuum states from a whispering gallery mode resonator[J]. Optica, 2019,6(11): 1375-1380.

[4] Mingxiao L, Lin C, Lue W, et al. Integrated Pockels laser[J]. Nature Communications,2022,13(1):5344-5344.

[5] Hung Y L, Danny E, Setareh G, et al.780 nm narrow-linewidth self-injection-locked WGM lasers[J].LASER RESONATORS, MICRORESONATORS, AND BEAM CONTROL XXII,2020,11266.

[6] Zhang W, Peng Y. Transmission characteristics of a Raman-amplified atomic optical filter in rubidium at 780 nm[J]. Journal of Optical Technology,2014,81(4):174-181.

[7] S S S, S B, E J D, et al.11 W narrow linewidth laser source at 780 nm for laser cooling and manipulation of Rubidium[J]. Optics express,2012,20(8):8915-9.

[8] T. Yabuki, T. Kita, Narrow Spectral Linewidth Wavelength Tunable Laser Diode using Self-injection Locking[J]. IEEE, 2023,pp. 1-2.

[9] V V S, L J E B, A D K, et al. Stabilizing DFB laser injection-locked to an external fiber-optic ring resonator[J]. Optics express,2020,28(1):478-484.

[10] R M F, D J S, Frank V. Whispering gallery mode sensors[J]. Advances in optics and photonics,2015,7(2):168-240.

[11] Jintian Lin, Fang Bo, Ya Cheng, Jingjun Xu. Advances in on-chip photonic devices based on lithium niobate on insulator[J]. Photonics Res.2020, 8(12):1910.

[12] Di Z, Linbo S, Mengjie Y, et al. Integrated photonics on thin-film lithium niobate[J]. ADVANCES IN OPTICS AND PHOTONICS, 2021,13(2):242-352.

[13] Zubov I F, Kryzhanovskaya V N, Moiseev I E, et al. Laser characteristics of an injection microdisk with quantum dots and its free-space outcoupling efficiency[J]. Semiconductors, 2016, 50(10): 1408-1411.

[14] Ting H, Yu M, Zhiwei F, et al. Wavelength-Tunable Narrow-Linewidth Laser Diode Based on Self-Injection Locking with a High-Q Lithium Niobate Microring Resonator[J]. Nanomaterials, 2 023, 13(5):948-948.

[15] J. Ling, J. Staffa, H. Wang, B. Shen, L. Chang, U. A. Javid, L. Wu, Z. Yuan, R. Lopez-Rios, M. Li, Y. He, B. Li, J. E. Bowers, K. J. Vahala, Q. Lin. Self-Injection Locked Frequency Conversion Laser[J]. Laser Photonics Rev,2023,17,2200663.

[16] Waclawek J P, Bauer V C, Moser H, et al.2f-wavelength modulation Fabry-Perot photothermal interferometry[J]. Optics Express, 2016.24(25): 28958-28967.

[17] Li S Y, Ngo N Q, Zhang Z R. Tunable Fiber Laser With Ultra-Narrow Linewidth Using A Tunable Phase-Shifted Chirped Fiber Grating [J]. IEEE Photonics Technology Letters, 2008, 20(17): 1482-1484.

[18] Huiqi L, Zhaocong W, Lei W, et al. Optically pumped Milliwatt Whispering-Gallery microcavity laser[J]. Light, science & applications,2023,12(1):223-223.

[19] Mian Z, Cheng W, Rebecca C, et al. Monolithic ultra-high-Q lithium niobate microring resonator[J]. Optica, 2017, 4(12): 1536-1536.

[20] M. N K, E. V L, E. A S, et al. Recent advances in laser self-injection locking to high-Q microresonators[J]. Frontiers of Physics, 2023,18(2):21305-.

[21] Zhenxu B, Zhongan Z, Yaoyao Q, et al. Narrow-Linewidth Laser Linewidth Measurement Technology [J]. Frontiers in Physics, 2021,9.

[22] Zhongan Z, Zhenxu B, Duo J, et al. Narrow laser-linewidth measurement using short delay self-heterodyne interferometry.[J].Optics express,2022,30(17):30600-30610.

[23] Dongdong W, Yanfei J, Han G, et al. Improvement and analysis of a recirculating delayed self-heterodyne interferometer for laser linewidth measurement[J].Optical Fiber Technology,2022,71.

[24] Chaoze Z, Ligang H, Tianyu G, et al. Laser coherence linewidth measurement based on deterioration of coherent envelope[J]. Optics and Laser Technology,2024,172110498-.

[25] Donati S. Developing self-mixing interferometry for instrumentation and measurements[J]. Laser & Photonics Reviews, 2012, 6(3): 393-417.

[26] Xiaolin L, Songqing Z, Xiaowu L, et al. Reflectivity measurement technology of special high reflective mirrors and uncertainty analysis of measurement results[J]. Optoelectronics Letters, 2023, 19(1): 49-54.

[27] M. N K, E. V L, V. A C, et al. Self-injection locking of a laser diode to a high-Q WGM microresonator[J]. Optics Express,2017,25(23): 28167-28167.